ELSEVIER

Cement & Concrete Composites 21 (1999) 223–232

Cement & Concrete Composites

Effects of fly ash on fatigue and fracture properties of hardened cement mortar

P.C. Taylor [a], R.B. Tait [b,*]

[a] Construction Technology Laboratories, 5420 Old Orchard Rd, Skokie, IL 60077-1030, USA

[b] Department of Mechanical Engineering, University of Cape Town, Private Bag, Rondebosch 7701, South Africa

Received 28 November 1997; accepted 16 November 1998

Abstract

The aim of the work described in this paper was to investigate the effects of fly ash on the fatigue resistance of cement mortars. Mortar mixes were prepared with similar compressive cube strengths using a range of fly ash contents up to 25%. Samples from these mixes were tested in a double torsion facility under cyclic loading and the rates of crack growth measured, recorded and plotted against the applied stress intensities on log–log scales in V–K diagrams. At later ages the fly ash was found to increase fatigue resistance and toughness. This was thought to be due to the spherical fly ash particles having a blunting effect. At greater ages the mixes containing fly ash were slightly less resistant to fatigue crack growth. Bond between the gel and the large fly ash particles was observed to be poor, resulting in their effectively acting as flaws that were now large in relation to other flaws in the matrix which had reduced with continued hydration.

Keywords: Fatigue; Fly ash; V–K curves

1. Introduction

Concrete has been the most significant building material for many generations, and has not lost its market dominance over the years. Despite the high energy consumption in cement manufacture, the total energy requirement to make a cubic metre of concrete is much lower than any other structural material. This also makes it very attractive in an age where energy conservation and environmental protection considerations are paramount. Furthermore the use of waste materials such as fly ash to modify the properties of concrete while at the same time reducing the proliferation of this potential pollutant also adds desirability to its use in concrete structures.

Considerable work has been reported [1–6] on the effects of fly ash when used as a partial cement replacement in concrete. Whole conferences [7–10] have been organised around fly ash, particularly on its effects on the potential durability of concrete.

On the other hand, durability is a subject that has largely been ignored in the past, but is becoming more and more important as large sums of money are being spent on concrete repair [11]. This has been partially due to changes in the composition of portland cement with time, with one of the major changes being the tendency to yield higher early strengths. This has lead to lower overall cement contents in concrete, but a consequent inadvertent increase in durability problems world wide.

A topic that is not durability related in the traditional sense, but certainly connected with structural serviceability, is that of fatigue. Fatigue is becoming increasingly important because economic and aesthetic pressures have promoted the use of increasingly slender structural sections, which in turn have been facilitated by the development of technologies able to meet such requirements. However, the more slender the section, the greater the relative effect of (cyclic) live load compared with dead load, and the greater the flexibility of the structure. All of these contribute to an increased risk of fatigue damage to cyclically loaded structures such as bridges and pavements as well as the burgeoning number of offshore structures [12].

This trend has accentuated the need for design codes that take cognisance of fatigue, and some such codes have been proposed [13–15]. Very little work has, however, been reported in which the effects of fly ash on

* Corresponding author. Tel.: +27-21-650-3249; fax: +27-21-650-3240; e-mail: meceng@engfac.ucf.ac.za

0958-9465/99/$ – see front matter
PII: S0958-9465(99)00005-0

fatigue or fracture toughness of concrete have been specifically investigated.

This paper describes work carried out in a research project that set out to evaluate the effect of fly ash on mortars subjected to cyclic, or fatigue, loading. The bulk of the work was in the form of fatigue tests and fracture toughness determinations using the double torsion technique, which is described in more detail below. It is accepted that linear elastic fracture analysis is not strictly applicable to mortars because of size effects. The use of the parameter K was considered to be acceptable in this case, however, where all samples were the same size, of similar strength and toughness and the results were used on a comparative basis. The compressive strength of the various mixes was also determined and an attempt was made to correlate performance with microstructural features of mortars using scanning electron microscopy. The details of the methods, materials, results and conclusions are presented in the following sections.

Table 1
Composition of cement and fly ash (as percentages by mass) with physical properties

	Portland cement	Fly ash
CaO	62.8	8.0
SiO_2	22.2	47.8
Al_2O_3	4.2	29.8
Fe_2O_3	2.7	4.0
MgO	2.2	2.2
SO_3	2.7	0.65
TiO_2	0.2	1.9
Mn_2O_3	0.3	–
P_2O_5	0.2	1.2
Na_2O	0.06	0.60
K_2O	0.44	0.75
L.O.I.	0.8	0.92
Free lime	0.8	–
Insoluble residue	0.3	2.2
Specific surface (m^2/kg)	471	–
Initial setting time (hours:minutes)	3:20	–
Final setting time (hours:minutes)	4:00	–
Expansion (%)	0	–
% passing 45-μm sieve	–	92.2

2. Experimental details

A series of tests were carried out using the double torsion method of measuring crack growth rates under constant stress intensities. The details of this technique are given below, following the discussion of materials selection, sample preparation and information on the other experimental parameters.

2.1. Materials and mix design

The use of mortars was selected in order to minimise the number of materials (i.e. variables) in the mixes and so reduce the variability incurred from including stone without incurring the problems associated with using paste such as shrinkage. It was also necessary to comply with thickness criteria pertaining to the test method by limiting aggregate size (see Refs. [16,17] for the background to these limits).

A rapid hardening portland cement (Type III) was obtained from a single batch from a local factory. A sample of fly ash was obtained from a single batch from Matla Power Station. The cement and fly ash were stored in airtight 200 litre drums. Analyses of the cement and the fly ash are given in Table 1.

A red siliceous pit sand (nominally 100% passing the 600-μm sieve) was used as aggregate. The material was commercially available and most closely approached the requirement that the maximum grain size should be less than 1/15th of the specimen thickness [16].

The aim of the mix design was to obtain similar compressive strengths (approximately 40 MPa) at seven days using three different proportions of fly ash, namely 0%, 15% and 25%. This approach was adopted in order to model engineering practice where compressive strength is the parameter normally specified. The ash contents were selected as those that were commonly used in practice.

The other targets were to have similar workability as determined by using a flow table [18], and similar sand contents. Again, following engineering practice, these parameters were considered more important than having constant water or cementitious contents. Final mix proportions were selected after trial mixes had been prepared, assessed and water/cement ratios modified to meet the criteria described above. The proportions used in the mixes used throughout the programme are given in Table 2.

2.2. Specimen preparation

Purpose made moulds were machined to the required sizes from sheets of clear perspex. Each mould held a batch of fifteen 225 × 75 × 8-mm specimens which were

Table 2
Mix proportions per cubic meter of mortar

	OPC (0% FA)	15% FA	25% FA
Cement (kg)	681	586	561
Fly ash (kg)	0	103	187
Sand (kg)	1145	1143	1078
Water (l)	341	328	325
Water/cementitious ratio	0.50	0.56	0.43
Aggregate/cementitious ratio	1.68	1.66	1.44

cast with the longest dimension vertical. The moulds were sized such that the top few millimetres of each specimen were cut off to remove mortar that was affected by bleeding.

The mould was clamped onto a running Vebe vibrator and was filled with the mixture by means of a purpose made square funnel that just fitted into the mould. Standard 50-mm cube moulds were used to form the samples for compression testing in a compression testing machine.

The filled moulds were left under plastic sheeting overnight, then stripped approximately 24 h after filling. The specimens were marked, placed into a curing tank filled with lime saturated water controlled at 25 ± 2°C and left in the tank (except for trimming) until removed for testing.

After four to seven days, the top 15 mm was cut off the DT specimens using a diamond tipped blade on a cutting table. The specimens were then notched at the top end for approximately one third of the length on the centre line in a rig made on a converted lathe that held the specimens straight and flat with respect to the blade. This was necessary because small out of true errors in the shape of the samples would result in skew cracks developing, thus invalidating the tests.

2.3. Double torsion test method

The specimen used in the double torsion test consists of a flat plate, with approximate proportions of 1:10:30 for the depth, width and length respectively, as shown in Fig. 1. A notch is cut from one end through the full depth for about one quarter of the length along the centre line.

At the edge at which the notch is started, four-point loading is applied as shown in Fig. 1 such that each half-beam is effectively loaded in torsion in opposite directions. The load points were spherical in order to minimise effects of friction. A crack tended to grow down the centre line of the specimen if the loads are applied perfectly symmetrically and square.

The stress intensity at the crack tip, for a constantly applied load, is constant as the crack grows for approximately the middle third to middle half of the length of the specimen [19–21].

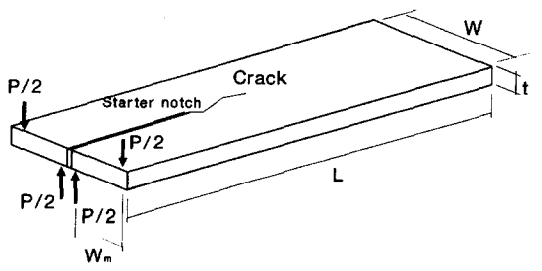

Fig. 1. The double torsion test specimen.

The relationship for calculating stress intensity was based on plane stress [21,22]:

$$K = P\, w_m \left(\frac{3(1+v)}{t^4 W \Psi} \right)^{1/2}, \tag{1}$$

where P is the applied load, w_m the distance between supports (moment arm), v the Poissons ratio, t the specimen thickness, W the specimen width, Ψ the thickness parameter as given below

$$\Psi = \left(1 - \frac{5}{4} \frac{t}{W} \right). \tag{2}$$

It is accepted that linear elastic fracture analysis is not strictly applicable to mortars because of size effects [23]. However, the use of the parameter K is considered to be acceptable in this case where all samples were of the same size, of similar strength and the results were used on a comparative basis [20].

One of the particular features of the DT system is that it effectively provides a constant K regime, independent of crack length [19–22]. Plots of load or stress intensity versus crack length should therefore nominally be constant and independent of crack length within the limits given above. The DT configuration is especially useful for fatigue studies as the rate of crack growth for a given load cycle, material and environment are also nominally constant. It is also useful because it is possible to change one of these parameters, for instance cyclic load amplitude or frequency, and to observe immediately the change (if any) in crack growth rate as a result, on a single specimen.

2.4. Test details

All the fatigue and toughness tests were conducted using an ESH servo-hydraulic machine that could be controlled in stroke or load control. Although the machine had a maximum load capacity of 50 kN, it was used with a 10 kN load cell on a full scale range of 1 kN, and was still accurate to 0.1% at this level. A signal generator with a sine wave output was used for the fatigue tests in load control over a range of frequencies from 0.1 to 20 Hz.

A purpose made test rig attached to the ESH was used throughout the program to provide the load configuration needed for the DT tests. The crack length measurement was achieved using a binocular microscope which was supported on a sliding mounting arm on a heavy base in the manner of a travelling microscope. The procedure used was to centre the crosshair on the observed crack tip and to use a vernier calliper to measure distance between the stops on the sliding arm and support arm of the microscope. The arrangement

was accurate to approximately 0.1 mm, which was as close as the actual crack tip could be judged. Readings were taken without stopping the cycling.

The technique of setting up the rig and the specimen was critical because any misalignment resulted in skew cracks, thus invalidating the test. Tolerances of a fraction of a millimetre were required to prevent wasted samples.

A DT specimen for fatigue testing was loaded by ramping in stroke control until the crack was observed to be in the field of view of the microscope. The load taken to achieve this was recorded and used as the basis for calculating the desired load amplitude as a percentage of the ultimate, and for determining the maximum stress intensity (K_{max}) for each sample. The machine was switched to load control and a cyclic load was then applied at the desired amplitude, frequency and maximum peak load.

At regular intervals a record was made of the number of cycles elapsed, the crack length, the maximum load and amplitude, as well as any comments and observations. Periodically the test parameters would be changed, thus allowing direct observation of their effect on the rate of fatigue crack growth in the specimen as indicated by the change of slope of the crack length versus number of cycles (a–N) curve.

The greatest difficulty in any given test, apart from the setting up, was the observation of the crack tip in order to measure the crack length. This is because cement mortars do not exhibit a single crack tip, but rather a zone with a number of cracks spreading out from the so called "crack tip", rather in the manner of a river tributary. However, in the measurement of crack growth rate, the absolute position of the "crack tip" need not be known, but only the position of some point a constant distance behind it. Therefore if a given technique was used consistently in a given specimen by the same observer identifying a point at which the crack was opening a given constant amount, then a reliable velocity could be measured satisfactorily.

The so called "ramp tests" involved the application of a constantly increasing downward displacement of the loading ram at a rate of 0.007 mm/s [23,24]. Whilst this displacement was applied, a record was kept of the load, deflection, time and crack length. In accordance with the theory [19,25], a plot of load versus time or crack length should increase up to a maximum, and then plateau at a constant load as the crack grew until just before failure. Other crack growth control means are possible, such as constant displacement or constant load, but these were not employed here.

For each test, the number of cycles and the length of the crack were plotted on a graph. The slope of the line was used to calculate, using a linear regression program, the crack velocity for a given set of test parameters and applied stress intensity.

The calculated velocities ($da/dt = V$) and applied stress intensities (K) were recorded; then plots of crack velocity (V) versus stress intensity (K) were generated on a log–log scale. The stress intensity referred to here is the maximum applied in the loading cycle. According to the literature [20] a typical V–K plot for materials subject to stress corrosion cracking is as shown in Fig. 2.

Typically, only the section marked I is observed in practice and is represented by the equation [19–22,25]

$$V = AK^n, \tag{3}$$

where A and n may be considered to be material constants.

Similar plots of the same results were also produced in which the stress intensities were normalised (K_{rel}) against the measured K_{max} determined in the ramp test on each sample ($K_{rel} = K/K_{max}$).

The factors that were varied during the course of the project (i.e. the matrix of experimental variables) were:

Percentage ash in the mix (%)	0 15 **25**
Specimen age at testing (days)	7 **28** 90 180
Cyclic load frequency (Hz)	0.1 **1** 5 10 20
Cyclic amplitude (% of ultimate load)	50 to 95
Maximum load (% of ultimate)	50 to 95 in steps of 5%

Not all possible combinations of the above variables were tested. A base set of those highlighted in **bold** above were selected, and then, in any given batch of specimens, one or two of the variables were changed within the ranges given.

3. Interpretation of results

Of particular interest in this paper are the VK results, and what can be inferred from them. Perhaps the most significant feature was that there is a large amount of inherent scatter in the results which arises from various sources.

Firstly, there is a large amount of scatter inherent in the double torsion test method, particularly when used

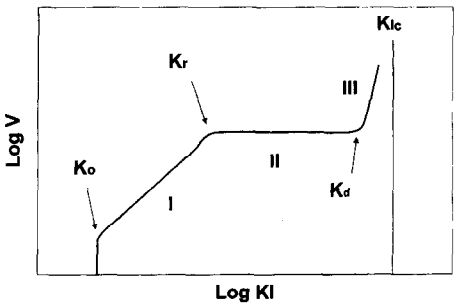

Fig. 2. Typical V–K curve for brittle materials.

to evaluate non-homogenous materials such as cement mortars.

This is further complicated in that the DT specimen can be used with a side groove or grooves to force the propagating crack to stay central. In the present case the specimens had no side grooves, which meant that cracks and microcracks could more readily bifurcate. Tait has reported [20,26] DT crack growth results on cement mortars but used a single groove on the compressive face, thus effectively forcing the propagating crack to remain single and symmetric. While this substantially reduces scatter, it is less representative of pure microcrack behaviour than the flat face specimens.

The implication of this was that the microcracks were very prone to bifurcation and branching. Fracture mechanics interpretations of crack growth rates, therefore, exhibited greater scatter because a number of cracks (rather than a single crack) required greater energy to drive them forward and slowed or stopped the apparent crack velocity. Data from samples in which more than one crack developed were discarded.

Secondly, the nature of fatigue itself also inherently leads to significant scatter, even in relatively clean metals and alloys, as microcracks need to initiate then propagate through individual grains. Suresh has also noted [27] that the amount of scatter in brittle materials subject to cyclic stresses is considerable.

These two effects together have lead to a wide scatter that has made interpretation of the results difficult. It should also be noted that this technique uses relatively "large" specimens in a mesostructural system, thus making interpretation of microstructural effects an exercise to be approached with care.

The policy that was adopted was to compare, on the various plots, the positions of the "clouds of data" with each other. In order to facilitate understanding, boundaries have been drawn around the clouds. In some cases the differences between these clouds have been of sufficient magnitude that it has been possible to infer that one set is distinct from another. In other cases the differences have been small enough to leave room for doubt about the influences of changing parameters on behaviour.

A cloud of data in a V–K plot that is above and to the left of another may be considered to exhibit less resistance to fatigue damage in that for a given applied stress intensity, a higher crack velocity has been indicated.

To draw firm inferences from the widely scattered data presented here is difficult as the correlation coefficients of best fit lines were poor; hence trend interpretation is generally better served using the "cloud of data" approach.

In following this approach, a different parameter is effectively being evaluated from that used by others [20,28]. If the equation of the best fit line is described by Eq. (1), then A and n are the material parameters to be compared. Conventionally it has been the slope of the line n (on a log–log scale) that has been the subject of discussion. If the *position* of clouds is the point of departure, then effectively it is the parameter A that is being compared.

The determination of n for the present data can be carried out in different ways. If a least squares approach is used to determine n the line shown in Fig. 3, for example, is obtained with a corresponding n value of 9. For the same data, a line drawn by eye through the cloud of data has an n value of 20.

The justification for this latter approach is that there is scatter in both the X and Y directions. It is reasonable then that a better estimate of the true position of the mean line would be obtained by considering that which passes through the "centre of gravity" of the data points with a direction such that the "second moment of area" of the cloud is minimised. This approach has been used before in double torsion work [21].

For the present work the n values obtained using the least squares approach were between 5 and 15 with an average of approximately 10. If the "eyeball" approach were used the n values would range from 15 to 25 with a mean of 20. These latter values are similar to those reported by Tait [26,20] and Bazant [24,28] for similar materials using DT and three-point-bend methods respectively.

The V–K plots have been presented in two forms; one using the applied stress intensity (K) in the X axis, and the other where the applied stress intensity has been normalised against the toughness (K_{max}) of individual specimens and expressed as a percentage (K_{rel}). The reasons for this are addressed in the discussion.

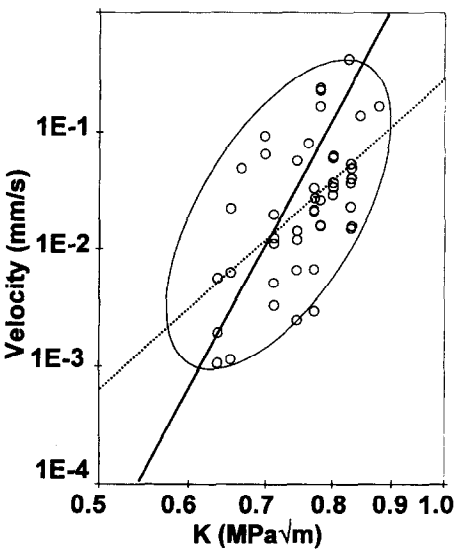

Fig. 3. A V–K plot showing a typical set of results along with the least squares best fit line (solid) and the "eyeball" best fit line (dashed).

4. Results

4.1. Specimen age

The compressive strengths of cubes from the three mixes are given in Fig. 4. This shows the similarity in 7- and 28-day strengths of all the mixes, and the greater strengths of the fly ash mixes at greater ages.

A typical set of results of fatigue tests on the effects of specimen age is presented in Fig. 5 in the form of V–K and V–K_{rel} plots for a 15% fly ash content.

It is of interest to note that there is little apparent difference between the 28 day and older sets, but the 7 day sets show a higher crack velocity for the same stress intensity. This is true for all fly ash contents on the V–K plots, but disappears when the data is presented as V–K_{rel}.

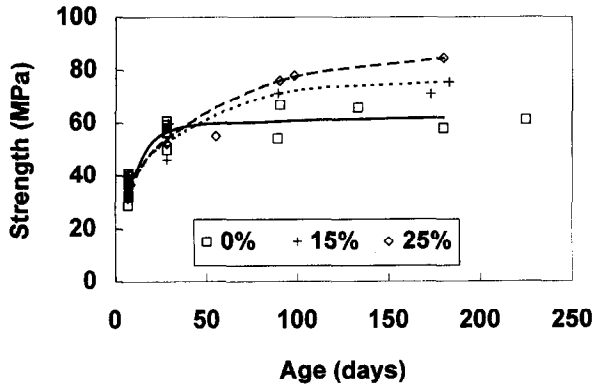

Fig. 4. Plot of the compressive strength results at various ages of the mixes with their different fly ash contents.

4.2. Fly ash content

If the above data is examined for the effect of fly ash content, the results are given sets of similar age showing the effect of the fly ash content. Figs. 6–8 give results for ages 7, 28 and 180 days respectively. At 7 and 28 days the OPC (0% fly ash) mix appears to have a similar crack velocity to that containing fly ash. However at greater ages the fly ash mix exhibits a faster (worse) crack velocity for the same applied stress intensity.

For the samples tested at an age of seven days, those containing fly ash exhibited a marginally slower crack growth rate than those with no fly ash (Fig. 6). At 28 days there did not appear to be any significant difference between the sets, whilst at 180 days the fly ash seemed to have a slight detrimental effect (Figs. 7 and 8). This is in agreement with work reported by Tait [29].

4.3. Toughness

The trends observed in the V–K plots for fatigue resistance described above were largely the same as those in the recorded values of toughness (K_{Ic}) as shown in Fig. 9.

There was a general increase in toughness with increasing fly ash content at 7 and 28 days but little effect of fly ash content at 90 and 180 days. With increasing age the toughness of all of the mixes increased with increasing hydration up to 90 days with little change between 90 and 180 days.

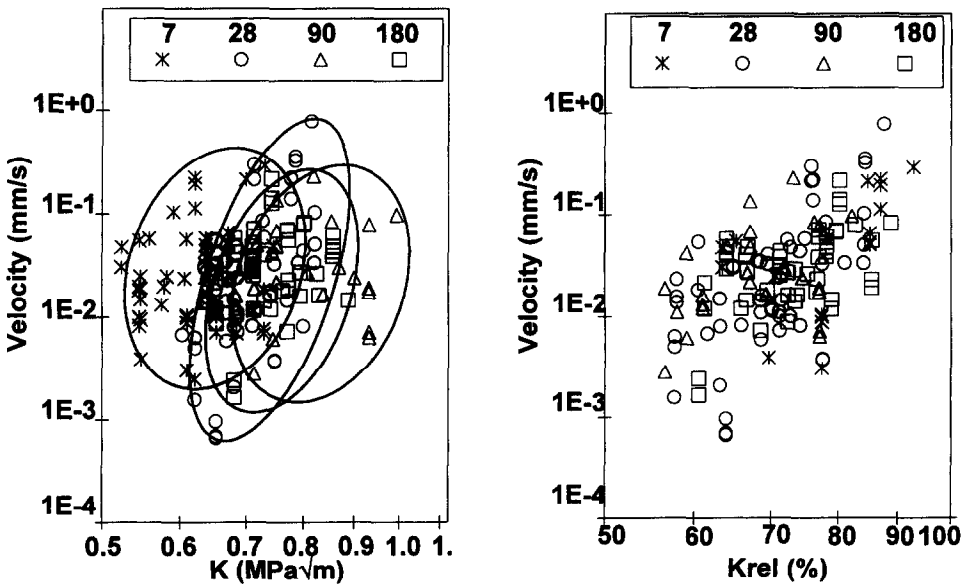

Fig. 5. V–K and V–K_{rel} plots for 15% fly ash showing the effect of sample age (in days).

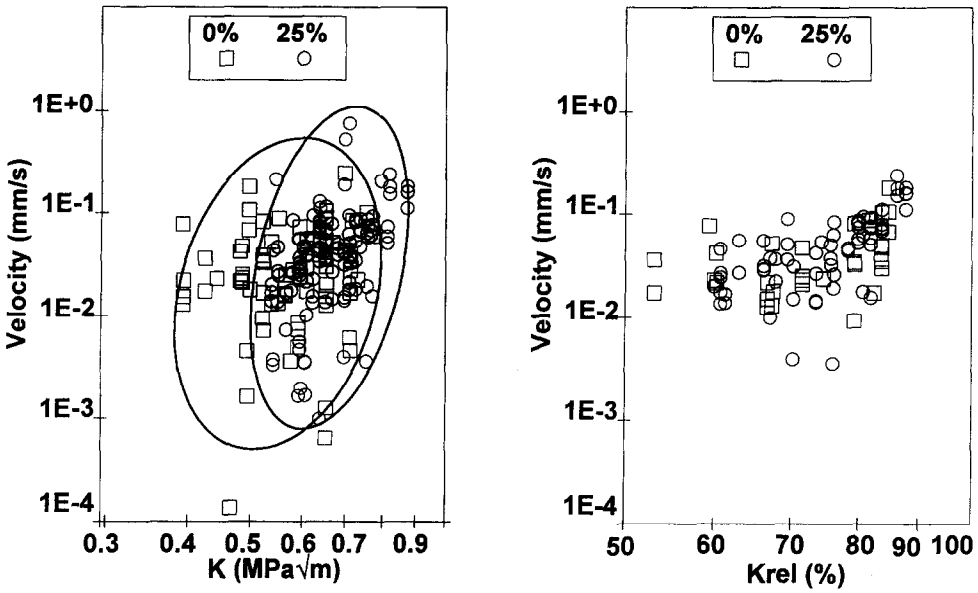

Fig. 6. *V–K* plot for 7 day old samples showing the effect of fly ash content.

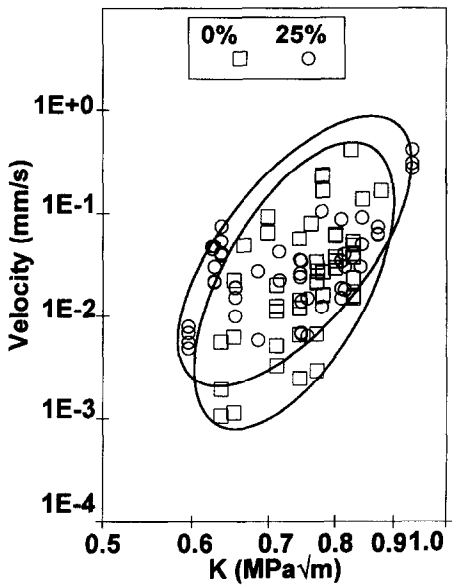

Fig. 7. *V–K* plot for 28 day old samples showing the effect of fly ash content.

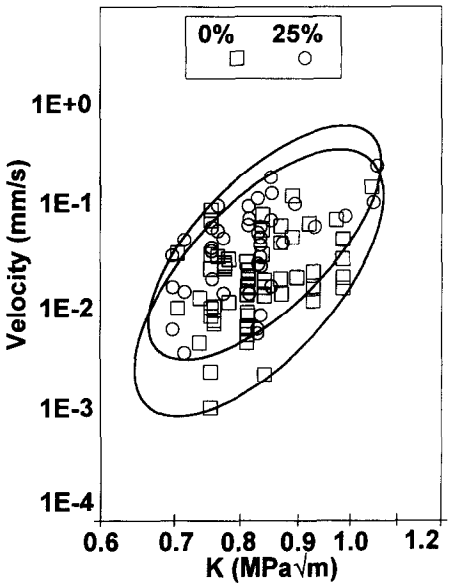

Fig. 8. *V–K* plot for 180 day old samples showing the effect of fly ash content.

5. Discussion

The discussion considers the present set of results in conjunction with those reported by other authors and leads to some conclusions about the fatigue behaviour and fracture mechanisms of cement mortar along with evaluation of the influences of fly ash content and specimen age on toughness and fatigue resistance, together with an attempt at a mechanistic explanation.

It has been noted that there was a closing up of differences in fatigue results when the data was normalised as K_{rel}, plots. This, and the similar trends observed in fatigue resistance and toughness, indicate that the fatigue characteristics of the family of materials tested in this project are broadly related to its toughness when considering variations due to age and fly ash content.

It can also be seen from Fig. 10 that at young ages cube strengths are independent of, but toughness varies with, changing fly ash content. However, at greater ages toughness is largely independent of, but strength varies

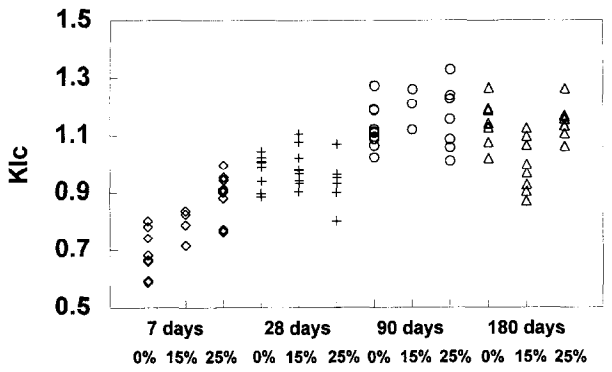

Fig. 9. K_{Ic} values of samples with different fly ash contents tested at various ages.

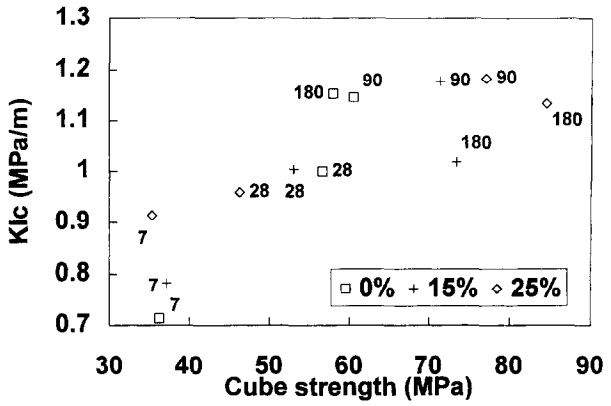

Fig. 10. A plot showing some K_{Ic} results against their respective cube strengths at various ages and fly ash contents.

with, fly ash content. This supports the contention that strength and toughness are not necessarily related for a given material.

As noted above, increasing fly ash content is beneficial to fatigue and toughness at early ages but slightly detrimental to fatigue resistance at greater ages (particularly if normalised against compressive strength). The magnitude of this effect is about 10% when comparing the applied load required to yield similar crack velocities. The cause of this behaviour is probably associated with the size and shape of the fly ash particles in relation to the size and shape of other flaws in the matrix as discussed below.

A limited amount of scanning electron microscopy was carried out to try to observe the microstructural changes in the samples due to the different binders used, and how these affected physical properties as a function of continued hydration with time, and the loads applied.

The micrographs (Figs. 11 and 12) show the development of hydration products, the increasing density of HCP and the increasing relative size of flaws induced by the fly ash compared with the rest of the paste.

The experimental SEM observations were consistent with those reported in the literature, all of which help to explain the fracture behaviour of cementitious materials in that:

- at early ages the paste contains a large number of voids that decrease in number and size with continued hydration;
- large fly ash particles do not bond well with the paste, even after some reaction, but create round flaws that can effect toughness depending on their size in comparison with other flaws in the paste. It should be

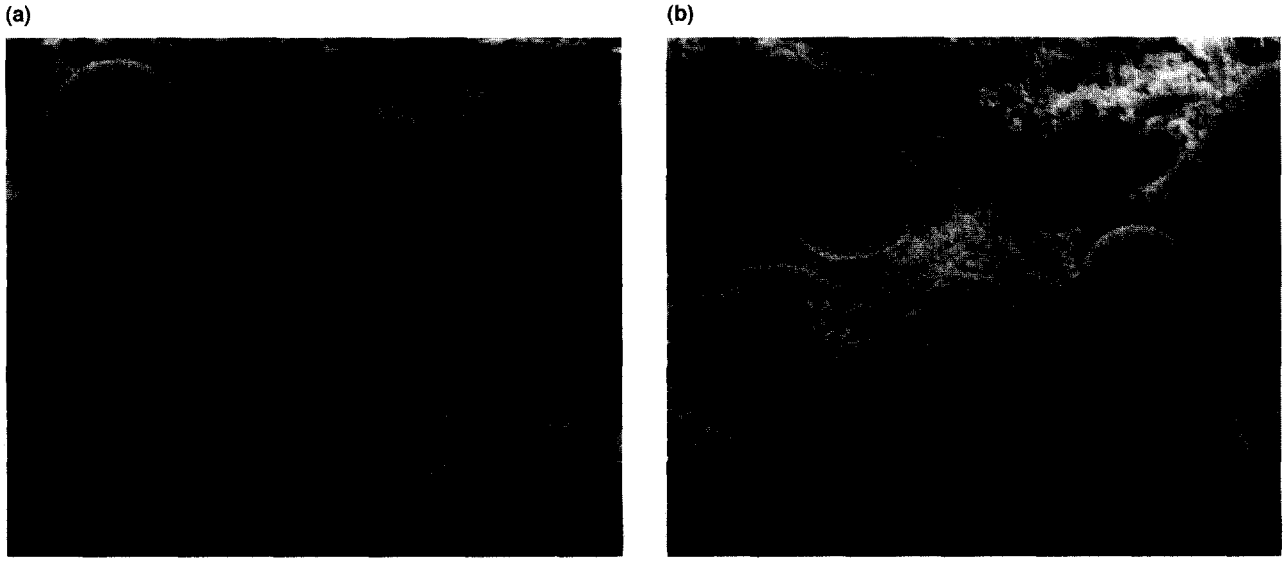

Fig. 11. After 7 days of hydration the matrix is dense and relatively few individual gel fibres can be seen.

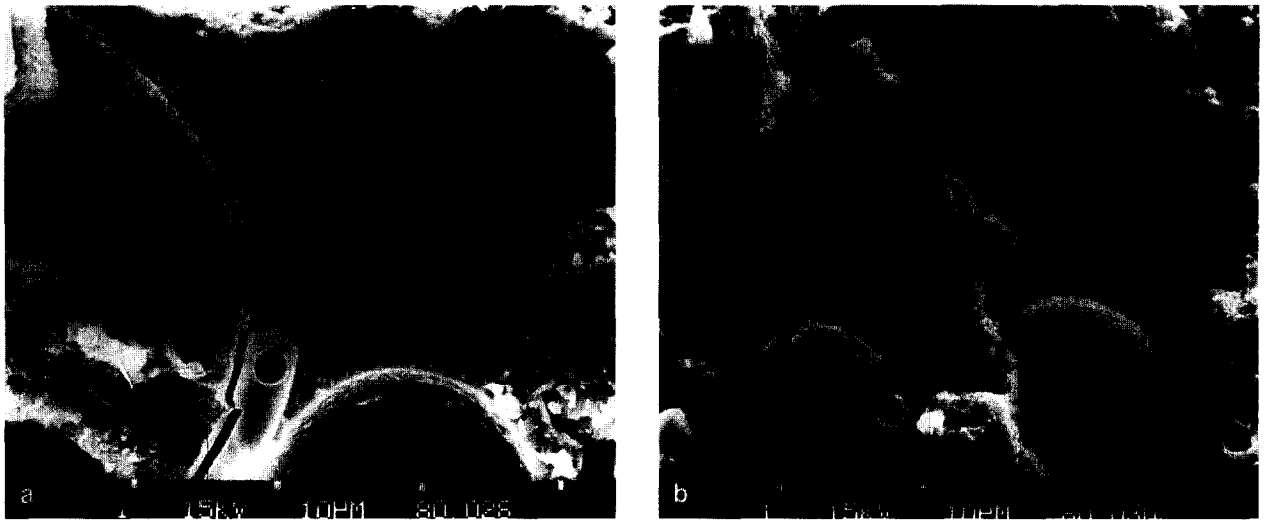

Fig. 12. After 8 months the matrix is very dense with the fly ash particles firmly embedded in it.

noted that even in old, well hydrated concretes, a significant amount of fly ash remains unreacted [30].

An overall impression gained from studying all of the micrographs was that the larger fly ash particles tended to be less reactive than the smaller, particularly at an early age, thus resulting in poor bond between the larger fly ash particles and the rest of the gel. At early ages, the size of the particles (and their associated flaws) is of the same order of magnitude as the other flaws in the paste, therefore they do not further reduce toughness to any marked degree. However, the shape of the fly ash flaw is such that a crack is impeded because the radius of the crack tip around the fly ash particle is large. Cracks have been observed to go around such flaws before being forced to split or stop, thus effectively toughening the material.

The reduction in-fatigue resistance with increasing fly ash content at greater ages is probably because many of the flaws in the paste reduce in number and magnitude with continued hydration, whilst those caused by the presence of large fly ash particles remain similar in size. These flaws therefore become *relatively* more significant and effectively reduce fatigue resistance when compared with the matrix without fly ash.

This concept of the relative importance (flaw magnitude and grain orientation) of the microstructure at the crack tip in influencing macro behaviour has similarly been expressed for metals by Miller [31].

There is a reported influence on fracture behaviour of cementitious materials due to the interfacial zone between paste and aggregate which may be modified by the presence of fly ash [32]. However, any beneficial influence of the very small fly ash particles reducing the effects of the interracial zone appears to have been masked, in this case, by the deleterious influence of the larger, less reactive, fly ash.

6. Concluding remarks

As noted in most of the above discussion, there is an apparent relationship between fatigue resistance and toughness for the materials tested.

The effects of fly ash and age point to the increasing toughness of mortar with increasing age and the toughening effect of fly ash particles at young ages when they are the same size as the rest of the flaws in the matrix, probably due to their shape. In addition, they appear to result in a detrimental effect on fatigue resistance when they are relatively large with respect to the other matrix flaws at greater ages.

References

[1] Davis RE et al. Properties of cements and concretes containing fly ash. Proceedings ACI 1937;33:577–612.
[2] Owens PL. Fly ash and its use in concrete. Concrete 1979;21–26.
[3] Ho DWS, Lewis RK. Effectiveness of fly ash for strength and durability of concrete. Cement & Concrete Research 1985;15(5):793–800.
[4] Tse EW, Lee DY, Klaiber FW. Fatigue behaviours of concrete containing fly ash, Fly Ash, silica fume and slag. Proceedings of the second international conference, Madrid, Spain, 1986;273–290 (ACI SP-91).
[5] Thomas MDA, Matthews JD. Durability studies of PFA concrete structures. BRE Information Paper, 11/91, June 1991.
[6] Dhir RK. A fundamental look at PFA. Concrete 1992:45–48.
[7] Symposium on the utilisation of pulverised fuel ash. CSIR, Pretoria, 1979.
[8] ASH – a valuable resource. Proceedings, Pretoria, CSIR, 1987:2–6.
[9] Fly ash, silica fume, slag, and natural pozzolans in concrete. Proceedings of the Fourth International Conference, Istanbul, Turkey, 1992 (ACI SP-132).
[10] Malhotra VM, editor. Fifth CANMET/ACI International Conference on Fly Ash, Silica Fume, Slag and Natural Pozzolans in Concrete, Milwaukee, June 1995, ACI.

[11] Dhir RK, Green JW, editors. Protection of concrete. Proceedings of the international conference held in Scotland. London: Spon, 1990.
[12] GC. Considerations for the use of concrete for offshore structures. Evaluation and rehabilitation of concrete structures and innovations in design, proceedings of an ACI international conference, Hong Kong, 1991;2:749–788 (ACI special publication 128).
[13] American Concrete Institute, Committee 215. Considerations for design of concrete structures subjected to fatigue loading (ACI 215R-74, revised 1992). ACI manual of concrete practice. Detroit: ACI, 1993;(part 1):215R-2–5.
[14] Portland Cement Association. Design of reinforced concrete for fatigue. Research & Development Bulletin RD 059.01 D, Skokie: PCA, 1978.
[15] Siemes AJM. Fatigue evaluation of concrete structures – preliminary studies, procedure and examples, Heron 1988;33(3).
[16] Hassanzadeh M, Hillerborg A. Theoretical analyses of test methods, SEM/Rilem international conference on fracture of concrete and rock, Houston, Texas 1987:388–95.
[17] Hillerborg A. Theoretical analysis of the double torsion test. Cement and Concrete Research 1983;13(1):69–80.
[18] 18ASTM C 109-92, Standard test method for compressive strength of hydraulic cement mortars. Philadelphia: American Society for Testing and Materials 1992:64–68.
[19] Tait RB, Fry PR, Garrett GG. Review & evaluation of the double torsion technique for fracture toughness and fatigue testing of brittle materials. Experimental Mechanics 1987:14–22.
[20] Tait RB. Fatigue and fracture of cement mortars. PhD Thesis, Cape Town, University of Cape Town, 1985.
[21] Witwatersrand, ch. 3, 1982:68–114.
[22] Fuller Jr. ER. An evaluation of double-torsion testing – analysis. Freiman SW, editor, Fracture mechanics applied to brittle materials. Philadelphia: American Society for Testing and Materials, 1979:3–18 (ASTM STP 678).
[23] Bazant ZP, Xu K. Size effect in fatigue fracture of concrete, ACI Materials Journal 1991;88(4):390–399.
[24] BS 5447:1977, Methods of test for plane strain fracture toughness (K_{Ic}) of metallic materials. London: British Standards Institution, 1977.
[25] Pletka BJ, Fuller Jr. ER, Koepke BG. An evaluation of double-torsion testing – experimental. Freiman SW, editor, Fracture mechanics applied to brittle materials. Philadelphia: American Society for Testing and Materials 1979:19–37 (ASTM STP 678).
[26] Tait RB, Garrett GG. A fracture mechanics evaluation of static and fatigue crack growth in cement mortar. Whittmann FH. editor. Fracture toughness & fracture energy of concrete. London: Elsevier, 1986:21–30.
[27] Suresh S. Fatigue of brittle solids, Chapter 13. Fatigue of materials. Cambridge: Cambridge University Press, 1991:435.
[28] Bazant ZP, Gettu R. Rate effects and load relaxation in static fracture of concrete. ACI Materials Journal 1992;85(5):456–468.
[29] Tait RB. Comparative slow crack growth behaviour in hardened cement paste containing PFA. ASH – A valuable resource, proceedings, CSIR, Pretoria 1987;2:2–6.
[30] ?tul=0>Dhir RK et al. Contribution of PFA to concrete workability and strength development. Cement & Concrete Research 1988;18(2):277–289.
[31] Miller KJ. Materials science perspective of metal fatigue resistance. Materials Science and Technology 1993;9:453–514.
[32] Saito M, Kawamura M. Effect of fly ash and slag on the interracial zone between cement and aggregate. Fly ash, silica fume, slag, and natural pozzolans in concrete, proceedings of the third international conference, Trondheim, Norway, 1989:669–88 (ACI SP-114).